

Document downloaded from:

<http://hdl.handle.net/10251/59303>

This paper must be cited as:

Jiménez Marco, A.; Sánchez González, L.; Desobry, S.; Chiralt Boix, MA.; Arab Tehrani, E. (2014). Influence of nanoliposomes incorporation on properties of film forming dispersions and films based on corn starch and sodium caseinate. *Food Hydrocolloids*. 35:159-169. doi:10.1016/j.foodhyd.2013.05.006.



The final publication is available at

<http://dx.doi.org/10.1016/j.foodhyd.2013.05.006>

Copyright Elsevier

Additional Information

1 **Influence of nanoliposomes incorporation on properties of film forming**
2 **dispersions and films based on corn starch and sodium caseinate.**

3 *Alberto Jiménez*¹, Laura Sánchez-González², Stéphane Desobry², Amparo Chiralt¹,*

4 *Elmira Arab Tehrani²*

5
6 ¹Instituto de Ingeniería de Alimentos para el Desarrollo. Departamento de Tecnología
7 de Alimentos. Universitat Politècnica de València. Camino de Vera s/n. 46022.
8 Valencia, Spain.

9 ²Laboratoire d'Ingénierie des Biomolécules (LIBio). ENSAIA - Université de Lorraine.
10 2 avenue de la Forêt de Haye, TSA 40602, 54518 Vandœuvre-lès-Nancy Cedex, France.

11
12
13 *(*) Contact information for Corresponding Author*

14 Instituto de Ingeniería de Alimentos para el Desarrollo. Universitat Politècnica de
15 València. Camino de Vera, s/n. 46022. Valencia. Spain.

16 Phone: 34-3877000 ext.83613, Fax: 34-963877369, e-mail: aljimar@upvnet.upv.es

17
18
19
20
21
22
23
24
25
26
27
28
29

30 **ABSTRACT**

31

32 The incorporation of potentially antimicrobial volatile compounds (orange essential oil
33 and limonene) into soy and rapeseed nanoliposomes was carried out by encapsulating
34 them through sonication of their aqueous dispersions. Nanoliposomes were added to
35 starch-sodium caseinate (50:50) film forming dispersions, which were dried to obtain
36 films without losses of the volatile compounds. Structural, mechanical and optical
37 properties of the films were analysed, as well as their antimicrobial activity against
38 *Listeria monocytogenes*. The addition of liposomes in the polymeric matrix supposed a
39 decrease of the mechanical resistance and extensibility of the films. The natural colour
40 of lecithin conferred a loss of lightness, a chroma gain and a redder hue to the films,
41 which were also less transparent than the control one, regardless the lecithin and volatile
42 considered. The possible antimicrobial activity of the films containing orange essential
43 oil or limonene was not observed, which could be due to their low antilisterial activity
44 or to the inhibition effect of the encapsulation which difficult their release from the
45 matrix.

46

47 **Keywords:** Starch-sodium caseinate films, nanoliposomes, antimicrobial,
48 encapsulation.

49

50

51

52

53

54

55

56

57

58

59

60

61

62

63

64 1. INTRODUCTION

65

66 Nowadays, it is well known that edible and biodegradable films obtained from
67 biopolymers are able to substitute, at least partially, conventional plastics. The
68 biodegradable plastics, after their useful life, get assimilated by microorganisms and
69 return to the natural ecosystem without causing any pollution or harm to the
70 environment (Maran, Sivakumar, Sridhar & Immanuel, 2013). Polysaccharides and
71 proteins are used in film formulations, since it is possible to obtain transparent,
72 tasteless, odorless and isotropic films by using these polymers (Chick & Ustunol, 1998;
73 Han, 2002; Soliva-Fortuny, Rojas-Graü & Martín-Belloso, 2012). In this sense, one of
74 the most used polysaccharide to obtain films with adequate properties is starch. This
75 biopolymer is a renewable resource, inexpensive (compared with other compounds) and
76 widely available (Lourdin, Della Valle & Colonna, 1995). Starch based films can be
77 formed by using its pure components (amylose and amylopectin; Paes, Yakiments, &
78 Mitchell, 2008), native starch (López & García, 2012), modified starches (López,
79 García & Zaritzky, 2008) and soluble or pregelatinized starch (Pagella, Spigno & De
80 Faveri, 2002). Nevertheless, starch films, as other polysaccharide films, are highly
81 sensitive to moisture action. Furthermore, their mechanical behaviour can vary as a
82 consequence of retrogradation phenomenon throughout time (Famá, Goyanes &
83 Gerschenson, 2007; Jiménez, Fabra, Talens, & Chiralt, 2012a)

84 The hydrophilic character of starch films can be modified by different techniques
85 such as surface sterification (Zhou, Ren, Tong, Xie, & Liu, 2009), surface
86 photocrosslinking (Zhou, Zhang, Ma, & Tong, 2008) or by adding hydrophobic
87 compounds to film formulation (Averous, Moro, Dole, & Fringant, 2000; Fang &
88 Fowler, 2003). On the other hand, starch retrogradation has been inhibited by mixing
89 starch with other polymers such as hydroxypropylmethylcellulose (HPMC) or sodium
90 caseinate (Jiménez, Fabra Talens & Chiralt, 2012b,c). Whereas starch-HPMC films
91 showed phase separation in the film, starch-sodium caseinate films were completely
92 homogeneous and showed good functional properties.

93 Biodegradable films are able to act as carriers of active compounds such as
94 antioxidants or antimicrobials to enlarge the self life of food products where they are
95 applied. Among these compounds, essential oils have a great relevance due to the fact
96 that they can act as antioxidants and antimicrobials at the same time (Ruiz-Navajas,
97 Viuda-Martos, Sendra, Perez-Alvarez, Fernández-López, 2013; Ye, Dai & Hu, 2013). In

98 general, essential oils are a mix of volatile (85-99 %) and non volatile compounds (1-15
99 %) (Sánchez-González, Vargas, González-Martínez, Cháfer & Chiralt, 2011a) in which
100 the volatile fraction is composed by terpens, terpenoids and other aromatic and aliphatic
101 components with low molecular weight (Smith-Palmer, Stewart, Fyfe, 2001; Bakkali,
102 Averbeck, Averbeck & Idaomar, 2008). Previous studies reported antimicrobial activity
103 of films containing different essential oils such as those obtained from bergamot
104 (Sánchez-González, Cháfer, Chiralt & González-Martínez, 2010a; Sánchez-González,
105 Cháfer, Hernández, Chiralt & González-Martínez, 2011b), lemon (Sánchez-González,
106 González-Martínez, Chiralt & Cháfer, 2010b; Iturriaga, Olabarrieta, Martínez de
107 Marañón, 2012) or sweet and bitter orange (Iturriaga *et al.*, 2012). However, isolate
108 terpenes (limonene, geranyl acetate and alpha-pinene) have been found to promote the
109 growth of *Listeria monocytogenes* in biofilms structures (Sandasi, Leonard & Viljoen,
110 2008), whereas the antimicrobial activity of essential oils has been attributed to the
111 synergism between different terpenes, which would improve their activity against
112 bacteria (Gallucci, Oliva, Casero, Dambolena, Luna, Zygodlo & Demo, 2009;
113 Piccirillo, Demiray, Silva Ferreira, Pintado & Castro, 2013) and fungi (Edris & Farrag,
114 2003).

115 Due to its volatile nature, essential oils can evaporate from film forming
116 dispersions during drying, thus reducing its effectiveness in dried films. The
117 encapsulation of essential oils could be a solution to maintain their usefulness for a
118 longer time, by a control release of the compounds. The encapsulation of a hydrophobic
119 compound in an aqueous dispersion requires the utilization of amphiphilic substances
120 such as lecithin. Recently Zhang *et al.* (Zhang, Arab Tehrany, Kahn, Ponçot, Linder &
121 Cleymand, 2012) have obtained very stable lecithin nanoliposomes by means of
122 sonication, in order to incorporate them in chitosan films.

123 The aim of this work was the development of starch-sodium caseinate films
124 containing nanoliposomes as carriers of antimicrobial compounds (orange essential oil
125 and D-limonene). The influence of the nanoliposomes addition with and without
126 antimicrobials in the properties of film forming dispersions (surface tension and
127 rheological properties) and films (mechanical, optical and antimicrobial properties) was
128 studied.

129

130 2. MATERIALS AND METHODS

131

132 **2.1. Materials**

133 Corn starch was purchased from Roquette (Roquette Laisa España, Benifaió,
134 Spain) and sodium caseinate (NaCas) was supplied by Sigma (Sigma–Aldrich Chemie,
135 Steinheim, Germany). Glycerol (99.5 % AnalaR NORMAPUR), chosen as plasticizer,
136 was provided by WVR International. To form nanoliposomes, rapeseed and soy
137 lecithins were obtained from The Solae Company (Solae Europe, Geneva, Switzerland)
138 and Novastell (Etrépany, France), respectively. Furthermore, D-Limonene stabilized
139 (purchased from Acros Organics, Geel, Belgium) and orange essential oil (supplied by
140 Laboratoires Mathe, Maxeville, France) were chosen as antimicrobial compounds.
141 BF₃(Boron trifluoride)/methanol (99 %) and chloroform (99.8%), used in gas
142 chromatography, were obtained from Bellfonte-PA (USA) and Prolabo-VWR (Italy)
143 respectively. Hexane (95%) and methanol (99.9%) were obtained from Carlo-Erab
144 (France) meanwhile acetonitrile (99.9%) was obtained from Sigma (Sigma–Aldrich
145 Chemie, Steinheim, Germany). These organic solvents were analytical grade reagents.

146

147 **2.2. Preparation and characterization of nanoliposomes**

148 Nanoliposomes were obtained by modifying the method of Zhang *et al.* (2012). 2 g
149 of lecithin were added in 38 g of distilled water and then stirred for 5 h. After this step,
150 the mixture was sonicated at 40 kHz and 40% power for 300 s (1 s on and 1 s off).
151 Sonication step was carried out by using a sonicator (Vibra Cell 75115, Bioblock
152 Scientific, Illkirch, France). In the case of formulations containing antimicrobials (2 g),
153 these compounds were added directly to the lecithin aqueous dispersions previously to
154 sonicate. The amount of antimicrobials (2 g) included in the formulations favoured their
155 proper retention in the nanoliposome core, avoiding their loss by evaporation.

156

157 **2.2.1. Fatty acids composition**

158 Fatty acid esters (FAMES) were prepared as described by Ackman (Ackman,
159 1998). The separation of the FAMES was carried out on a Shimadzu 2010 gas
160 chromatograph Perichrom (Saulx-lès-Chartreux, France), equipped with a flame-
161 ionization detector. A fused silica capillary column was used (60 m, 0.2 mm i.d. ×0.25
162 µm film thicknesses, SPTM2380, Supelco, Bellefonte, PA, USA). Injector and detector
163 temperatures were set at 250 °C. A temperature program of column initially set at 120
164 °C for 3 min, then rising to 180 °C at a rate of 2 °C/min and held at 220 °C for 25 min.
165 Standard mixtures (PUFA1, from marine source, and PUFA2, from vegetable source;

166 Supelco, Sigma–Aldrich, Bellefonte, PA, USA) were used to identify fatty acids. The
167 results were presented as triplicate analyses.

168

169 **2.2.2. Lipid classes**

170 The lipid classes of the different fractions were determined by Iatroscan MK-5
171 TLC-FID (Iatron Laboratories Inc., Tokyo, Japan). Each sample was spotted on ten
172 Chromarod S-III silica coated quartz rods held in a frame. The rods were developed
173 over 20 min in hexane/diethyl ether/formic acid (80:20:0.2, v:v:v), then oven dried for 1
174 min at 100 °C and finally scanned in the Iatroscan analyzer. The Iatroscan was operated
175 under the following conditions: flow rate of hydrogen, 160 ml/mn; flow rate of air, 2
176 L/mn. A second migration using a polar eluant of chloroform, methanol, and ammoniac
177 (65:35:5) made it possible to quantify polar lipids. The FID results were expressed as
178 the mean value often separate samples. The following standards were used to identify
179 the sample components:

180 -Neutral lipids: 1-monostearoyl-rac-glycerol, 1,2-dipalmitoyl-snglycerol, tripalmitin,
181 cholesterol.

182 -Phospholipids: L- α -phosphatidylcholine, 3 sn-phosphatidylethanolamine, L- α -
183 phosphatidyl-L-serine, L- α -phosphatidylinositol, lyso-phosphatidylcholine,
184 sphingomyelin.

185 All standards were purchased from Sigma (Sigma–Aldrich Chemie, Steinheim,
186 Germany. The recording and integration of the peaks were provided by the ChromStar
187 internal software.

188

189 **2.2.3. Nanoliposomes size measurement**

190 Size of nanoliposomes was determined by using a Malvern Zetasizer Nano ZS
191 (Malvern Instruments, Worcestershire, U.K.) considering the method of Zhang *et al.*
192 (2012). Samples were diluted in distilled water (1:100) and measured at 25 °C. At least
193 five replicates were considered for each formulation.

194

195 **2.2.4. Electrophoretic mobility**

196 Electrophoretic mobility of nanoliposomes was measured in the aqueous dispersion
197 by means of a Malvern Zetasizer Nano ZS (Malvern Instruments, Worcestershire, UK)
198 at 25 °C. Dispersions were diluted to a particle concentration of 0.01 % using deionised
199 water.

200

201 **2.2.3. Surface tension**

202 Surface tension of nanoliposomes aqueous dispersions (and film forming
203 dispersions) was measured by using a Krüss K100 tensiometer (Krüss GmbH;
204 Hamburg, Germany) equipped with a platinum plate. All measures were taken in
205 triplicate at 25 °C.

206

207 **2.3. Preparation and characterization of film forming dispersions**

208 Seven different film forming dispersions based on corn starch, sodium caseinate
209 and glycerol as plasticizer were prepared. Corn starch was dispersed in cool water to
210 obtain 2 % (w/w) polysaccharide dispersions. These were maintained, under stirring, at
211 95 °C for 30 min to induce starch gelatinization. Sodium caseinate was dissolved
212 directly in cool distilled water (2 % w/w). Afterwards, both hydrocolloids were mixed
213 to obtain dispersions with a starch:protein ratio of 1:1. This ratio was used on the basis
214 of a previous study carried out by Jiménez *et al.* (2012c) who observed no starch
215 crystallization in this mixture. After this step, a controlled amount of glycerol was
216 added (hydrocolloid:glycerol ratio was 1:0.25). In the case of dispersions containing
217 nanoliposomes, 10 g of nanoliposome solution were added to 90 g of hydrocolloid
218 dispersions. Then the mixtures were maintained 1 hour under stirring at 300 rpm to
219 disperse nanoliposomes.

220

221 **2.3.1. Rheological behaviour**

222 The rheological behaviour of the film forming dispersions was analyzed in
223 triplicate at 25 °C by means of a rheometer (Malvern Kinexus, Malvern Instruments,
224 Worcestershire, U.K.) with a coaxial cylinder sensor. Flow curves were obtained after
225 resting the sample in the sensor for 5 min at 25 °C. The shear stress (σ) was measured as
226 a function of shear rate ($\dot{\gamma}$) from 0 to 1000 s⁻¹ and up and down curves were obtained.
227 When samples showed non-Newtonian behaviour, the power law model was applied to
228 determine the consistency index (k) and the flow behaviour index (n).

229

230 **2.4. Preparation and characterization of films**

231 Films were obtained by casting. Film forming dispersions were gently poured
232 (88.84 g of solids/m²) over PET Petri dishes (85 or 140 mm diameter) resting on a
233 leveled surface. The dispersions were allowed to dry for approximately 48 h at 45 %

234 RH and 20 °C. Dry films could be peeled intact from the casting surface. Seven kinds of
235 films were prepared: without nanoliposomes (control), with lecithin nanoliposomes
236 (Rap or Soy), with limonene-lecithin nanoliposomes (Rap-lim or Soy-lim) and with
237 essential oil-lecithin nanoliposomes (Rap-oil or Soy-oil).

238 **2.4.1. Film conditioning**

239 Before tests, all samples were conditioned in a desiccator at 25 °C and 53 % RH,
240 by using magnesium nitrate-6-hydrate saturated solutions (Sigma–Aldrich Chemie,
241 Steinheim, Germany) for one week, when the analyses were carried out.

242

243 **2.4.2. Mechanical properties**

244 A Lloyd instruments universal testing machine (AMETEK, LRX, U.K.) was used
245 to determine the tensile strength (TS), elastic modulus (EM), and elongation (E) of the
246 films, according to ASTM standard method D882 (2001). EM, TS, and E were
247 determined from the stress-Hencky strain curves, estimated from force-distance data
248 obtained for the different films (2.5 cm wide and 10 cm long). At least four replicates
249 were obtained for each formulation. Equilibrated film specimens were mounted in the
250 film-extending grips of the testing machine and stretched at a deformation rate of 50
251 mm/min until breaking. The relative humidity of the environment was held constant at
252 53 % during the tests, which were performed at 25 °C.

253 Measurements of film thickness were carried out by using an electronic digital
254 micrometer (0–25 mm, 1 µm).

255

256 **2.4.3. FTIR analysis of films**

257 Fourier transform infrared spectroscopy was used to study the presence of
258 interactions between components in conditioned films in total attenuated reflection
259 mode (ATR-FTIR). Measurements were carried out at 25 °C by using a Tensor 27 mid-
260 FTIR Bruker spectrometer (Bruker, Karlsruhe, Germany) equipped with a Platinum
261 ATR optical cell and an RT-D1a TGS detector (Bruker, Karlsruhe, Germany). The
262 diaphragm during analysis was set at 4 mm whereas the scanning rate was 10 kHz. For
263 the reference (air) and each formulation 154 scans were considered from 4000 to 800
264 cm^{-1} , with a resolution of 4 cm^{-1} .

265 After measurements, data were treated by using OPUS software (Bruker,
266 Karlsruhe, Germany). Initial absorbance spectra were smoothed using a nine-points

267 Savitsky-Golay algorithm as well as elastic baseline correction (200 points) was applied
268 to spectra. These were then centered and normalized using the mentioned software.

269

270 **2.4.4. Optical Properties**

271 To evaluate the films transparency, the Kubelka-Munk theory was considered for
272 multiple scattering to the reflection spectra (Hutchings, 1999). When the light passes
273 through the film, it is partially absorbed and scattered, which is quantified by the
274 absorption (K) and the scattering (S) coefficients. Internal transmittance (Ti) of the
275 films was quantified using Equation 1. In this equation R_0 is the reflectance of the film
276 on an ideal black background. a and b parameters are calculated by Equations 2 and 3
277 where R is the reflectance of the sample layer backed by a known reflectance (R_g). The
278 surface reflectance spectra of the films were determined from 400 to 700 nm with a
279 spectrophotometer CM-5 (KonicaMinolta Co., Tokyo, Japan) on both a white and a
280 black background. All measurements were performed at least in triplicate for each
281 sample on the free film surface during its drying.

282

$$283 \quad T_i = \sqrt{(a - R_0)^2 - b^2} \quad \text{Equation 1}$$

284

$$285 \quad a = \frac{1}{2} \cdot \left(R + \frac{R_0 - R + R_g}{R_0 R_g} \right) \quad \text{Equation 2}$$

286

$$287 \quad b = (a^2 - 1)^{1/2} \quad \text{Equation 3}$$

288

289 Colour coordinates of the films, L^* , C_{ab}^* (Equation 4) and h_{ab}^* (Equation 5) from
290 the CIELAB colour space were determined, using D65 illuminant and 10° observer and
291 taking into account R_∞ (Equation 6) which correspond with the reflectance of an
292 infinitely thick layer of the material.

293

$$294 \quad C_{ab}^* = \sqrt{a^{*2} + b^{*2}} \quad \text{Equation 4}$$

295

$$296 \quad h_{ab}^* = \arctg\left(\frac{b^*}{a^*}\right) \quad \text{Equation 5}$$

297

298

$$R_{\infty} = a - b$$

Equation 6

299

300 Finally, to evaluate the colour differences between the different films and control
301 film, Equation 7 was used.

302

303

$$\Delta E = \sqrt{(\Delta L^*)^2 + (\Delta a^*)^2 + (\Delta b^*)^2}$$

Equation 7

304

305 **2.4.5. Scanning Electron Microscopy (SEM)**

306

307 Microstructural analysis of the films was carried out by SEM using a scanning
308 electron microscope (Hitachi S-4800, Japan). Film samples were maintained in a
309 desiccator with P₂O₅ for two weeks to ensure that no water was present in the sample.
310 Then, films were frozen in liquid N₂ and cryofractured with a pre-chilled razor to
311 observe the cross-section of the samples. Fractured film pieces were then mounted on a
SEM tube and observed using an accelerating voltage of 10 kV.

312

313 **2.4.6. Microbiological analysis**

314

315 To perform the microbiological analysis, a modification of the method proposed by
316 Kristo, Koutsoumanis & Biliaderis (2008) was considered. *Listeria monocytogenes* (CIP
317 82110), supplied by the Collection Institut Pasteur (CIP, France), was regenerated (from
318 a culture stored at -80 °C) by transferring a loopful of bacteria into 10 ml of Tryptone
319 Soy Broth-Yeast Extract, (TSB-YE, Biokar Diagnostics, Beauvais, France) and
incubating at 37 °C overnight. Subsequently, a 10 µl aliquot from the overnight culture
320 was then transferred to 10 ml of TSB-YE and grown at 37 °C until the end of the
321 exponential phase of growth. This culture, appropriately diluted, was then used for
322 inoculation of the agar plates in order to obtain a target inoculum of approximately 10³
323 CFU/cm². Tryptone soy agar (TSA, Biokar Diagnostics, Beauvais, France) was used as
324 a model solid food system. Aliquots of TSA (20 g) were poured into Petri dishes. After
325 the culture medium solidified, diluted overnight culture was inoculated on the surface.

326

327

328

329

The different test films of the same diameter as the Petri dishes (containing or not
nanoliposomes) were placed on the inoculated surface. Inoculated and uncoated TSA
Petri dishes were used as control. Petri dishes were then covered with parafilm to avoid
dehydration and stored for 7 days at 10 °C.

330 Microbial counts on Palcam agar base (Biokar Diagnostics, Beauvais, France)
331 plates were examined immediately after the inoculation and after 1, 4 and 7 days of
332 storage. To this end, the agar was removed aseptically from Petri dishes and placed in a
333 sterile plastic bag with 100 ml of Tryptone salt broth (Biokar Diagnostics, Beauvais,
334 France). The bag was then homogenized for 150 s in a Stomacher blender 400
335 (Interscience, Saint-Nom-La-Breteche, France). Serial dilutions were made and poured
336 onto Palcam agar base. The dishes were incubated during 24 h at 37 °C before colonies
337 were counted. All tests were performed in duplicate.

338

339 **2.5. Statistical Analysis**

340 Statgraphics Plus for Windows 5.1 (Manugistics Corp., Rockville, MD) was used
341 for carrying out statistical analyses of data through analysis of variance (ANOVA).
342 Fisher's least significant difference (LSD) was used at the 95% confidence level.

343

344 **3. RESULTS AND DISCUSSION**

345

346 **3.1. Characteristics of nanoliposomes**

347 **3.1.1. Fatty acids analyses**

348 The main fatty acid composition is shown in Table 1. The percentage of total
349 polyunsaturated fatty acids was the highest in soy lecithin. The high proportions of fatty
350 acids were C18:2 n-6 (52.27 %), found in the polyunsaturated fatty acids class, C18:1 n-
351 9 (21.49 %) in the monounsaturated fatty acids class and C16:0 (17.07 %) in the
352 saturated fatty acids class for soy lecithin. The largest amount of fatty acid was a
353 monounsaturated fatty acid, in regards to rapeseed lecithin, the percentage of C18:3n-3
354 (6.60 %) was important in the polyunsaturated fatty acids class. The fatty acid most
355 present was C18:1n-9 (56.51 %) found in the monounsaturated fatty acids class.

356

357 **3.1.2. Lipid classes**

358 The lipid classes of lecithins were separated by thin-layer chromatography
359 (Iatroscan). Moreover, the percentage of triacylglycerols (TAG) contained in lecithins
360 were respectively 37.75 ± 0.1 and $18.15 \pm 0.2\%$ for rapeseed and soy lecithins. However,
361 the percentage of polar fraction showed that soy lecithin was richer in polar lipids with
362 $84.76 \pm 0.6\%$ which was $62.26 \pm 0.8\%$ for rapeseed lecithin.

363

364 **3.1.3. Size of nanoliposomes**

365 The size analysis of nanoliposomes is of interest because of its impact on different
366 properties of the films and its stability and capacity to release the entrapped compounds
367 in the liposome core. Different authors (Pérez-Gago & Krochta, 2001; Bravin, Peressini
368 & Sensidoni, 2004) have related the particle size of lipids in the film forming emulsions
369 with different properties of the films such as mechanical or barrier properties. Low
370 particle size is generally desired since small particles increase the tortuosity of the
371 structure thus improving the barrier capacity and provides a more homogeneous
372 structure. The particle size of nanoparticles (or nanoliposomes) has to be controlled
373 since they can be toxic for humans and for the environment. In this sense, different
374 authors estimated the toxicity of different nanoparticles such as silver nanoparticles
375 (Lankveld, Oomen, Krystek, Neigh, Troost-de Jong, Noorlander, Van Eijkeren,
376 Geertsma, De Jong, 2010), TiO₂ nanoparticles (Clément, Hurel, Marmier, 2013) or ZnO
377 nanoparticles (Hsiao & Huang, 2011). Unfortunately, there are no works concerning the
378 toxicity of active compounds loaded-nanoliposomes.

379 The mean particle diameter of rapeseed and soy nanoliposomes without and with
380 antimicrobial compounds is showed in Table 2. The obtained values are in the same
381 order as those found by Zhang *et al.* (2012) and differences may be related with the
382 different time of sonication. They obtained stable nanoliposomes by using 180 s of
383 sonication whereas 300 s of sonication were necessary to incorporate completely the
384 antimicrobials into the nanoliposomes in this case.

385 Size of rapeseed nanoliposomes ranged between 146 and 150 nm without
386 significant differences between them. However, soy nanoliposomes showed different
387 sizes depending on the core compounds. Antimicrobial loaded-nanoliposomes showed
388 lower sizes. The addition of hydrophobic compounds seemed to favour the compactness
389 of soy nanoliposomes by improving the orientation of amphiphilic molecules of soy
390 lecithin through the interactions with the oil compounds. Previous studies (Zhang *et al.*,
391 2012) showed the formation of vesicles for the major part of lecithin molecules (soy and
392 rapeseed) with some remanent droplets, when applying sonication in water dispersion in
393 similar conditions. So, the formation of vesicles can be expected in this case, although
394 the incorporation of the essential oil or limonene could imply the formation of a
395 different structure due to the change in the balance of the interaction forces in the
396 mixture. Spherical micelles could entrap in their core the incorporated non-polar
397 compounds and a reduction in their size can occur.

399 **3.1.4. Electrophoretic mobility**

400 The electrophoretic mobility values of soy and rapeseed nanoliposomes containing
401 solutions are shown in Table 2. The study of the surface charge of the particles is of
402 interest since it affects the stability of the nanoliposomes, specially in the studied
403 solutions in which the viscosity is too low. The electrophoretic mobility of
404 nanoliposomes containing solutions ranged between -3.21 and $-3.36 \mu\text{m}\cdot\text{cm}\cdot\text{V}^{-1}\cdot\text{s}^{-1}$ for
405 rapeseed nanoliposomes and between -3.89 and $3.99 \mu\text{m}\cdot\text{cm}\cdot\text{V}^{-1}\cdot\text{s}^{-1}$ for soy
406 nanoliposomes. These values are in agreement with values reported by Zhang *et al.*
407 (2012). According with obtained results and those found by Arab Tehrany, Kahn,
408 Baravian, Maherani, Belhaj, Wang & Linder (2012), rapeseed and soy lecithins contain
409 different type of phospholipids such as phosphatidylserine, phosphatidic acid,
410 phosphatidylglycerol, phosphatidylinositol, phosphatidylcholine and
411 phosphatidylethanolamine. These components are negatively charged at neutral pH
412 (except phosphatidylcholine which is not charged) thus being responsible of the negative
413 electrophoretic mobility of liposomes (Chansiri, Lyons, Patel & Hem, 1999). The
414 incorporation of the essential oil and limonene slightly increase the particle charge
415 which agrees with the induced changes in the micellar structure.

416

417 **3.1.5. Surface tension of nanoliposomes dispersions**

418 Lecithins were chosen since its amphiphilic nature allows to incorporate the
419 hydrophobic antimicrobials into the hydrophilic starch-sodium caseinate dispersions.
420 Due to its low molecular weight, these surfactants migrate rapidly to the small terpen
421 droplets that are formed during sonication thus preventing coalescence and flocculation
422 (McSweeney, Healy & Mulvihill, 2008). Surface tension values of rapeseed and soy
423 nanoliposomes containing solutions are showed in Table 2. As expected, the surface
424 tension of nanoliposomes solutions was lower in comparison with pure water whose
425 surface tension is $72 \text{ mN}\cdot\text{m}^{-1}$ (Walstra, 2003). The obtained values demonstrate the
426 ability of lecithins to form stable nanoliposomes with and without antimicrobials in the
427 aqueous media. Differences in the surface tension values of the dispersions of rapeseed
428 and soy nanoliposomes were found. The surface tension of rapeseed nanoliposomes was
429 lower than for soy nanoliposomes containing solution. This fact can be associated to the
430 total content of polyunsaturated fatty acids (PUFA) with different surface activity. In
431 this sense, as showed in Table 1, the content of PUFA was higher in soy lecithin than in

432 rapeseed lecithin. Leshem, Landau & Deutsch (1988) related the presence of
433 unsaturations with an important effect on the surface tension. They explained that for a
434 fixed surfactant monolayer area in a completely expanded state, an increase in the
435 number of cis-double bonds cause an increase in the surface tension, in agreement with
436 results found in this work.

437 The inclusion of orange essential oil and D-limonene did not produce any
438 difference in surface tension for rapeseed nanoliposomes. However, the addition of
439 these compounds significantly reduced the surface tension of soy nanoliposomes
440 containing solutions. This indicates that the addition of these compounds affects the
441 critical micellar concentration and the corresponding minimal surface tension of the soy
442 lecithin. The lower value of the surface tension of rapeseed lecithin with respect to the
443 soy lecithin could be explained, as commented on above, by its lower concentration of
444 PUFA.

445

446 **3.2. Characterization of the film forming dispersions**

447 **3.2.1. Surface tension**

448 Table 3 shows the values of the surface tension of all film forming dispersions
449 under study. The presence of the protein in combination with starch remarkably reduced
450 the surface tension of water ($72 \text{ mN}\cdot\text{m}^{-1}$ at $25 \text{ }^\circ\text{C}$; Walstra, 2003) to $51.1 \text{ mN}\cdot\text{m}^{-1}$ as it
451 can be observed for control formulation. This effect is due to the amphiphilic nature of
452 caseinate and is in agreement with the results found by Fabra, Jiménez, Atarés, Talens
453 & Chiralt (2009). The analysis of the surface tension of film forming dispersions are of
454 interest, specially in the food industry, since low values of surface tension would favour
455 the coating of products (Fernández, Díaz de Apodaca, Cebrián, Villarán & Maté, 2006).
456 In the case of film forming dispersions containing nanoliposomes, the surface tension
457 was always lower as compared with the control sample as it was expected by the action
458 of surfactants. Nevertheless, the values did not reach those obtained in the aqueous
459 nanoliposome dispersions, which indicates that protein is present to a great extent in the
460 water-air interface and no total substitution of this occurred when nanoliposomes were
461 added. No notable differences were found between the different formulations with and
462 without antimicrobials, except for the film forming dispersion with soy-orange oil
463 nanoliposomes where the lowest surface tension was obtained. The greater migration of
464 surfactant to the sample surface seems to occur, thus decreasing the surface tension to a
465 greater extent. This fact could be related with a lower stability of liposomes in this case.

466

467 **3.2.2. Rheological behaviour**

468 The study of the rheological behaviour of film forming dispersions is of interest to
469 have information about the fluid structure and interactions between particles during
470 flow. The analyses of the rheological behaviour of the film forming dispersions were
471 carried out at 25 °C with a shear rate between 0 and 1000 s⁻¹. All formulations showed
472 newtonian behaviour at low shear rates and a shear thickening or dilatant character from
473 a determined shear rate (see Figure 1). Furthermore, all samples showed non-time
474 dependent behaviour since up and down curves coincided. The change in the
475 rheological behaviour as the shear rate increases can be related with particles (starch
476 and sodium caseinate chains and vesicles) aggregation due to orthokinetic flocculation
477 (Peker & Helvaci, 2007). The aggregates would present sufficient cohesive forces to
478 withstand the shear stress, thus producing shear thickening behaviour (Christianson &
479 Bagley, 1983). The water content entrapped in these aggregates would increase, leading
480 to a greater flow resistance.

481 The viscosity of studied film forming dispersions in the newtonian domain are
482 showed in Table 3. The obtained viscosities are low, in agreement with the polymer
483 concentrations used, thus indicating that no gels were formed during the film forming
484 dispersions preparation. Although starch-sodium caseinate interactions can take place in
485 determined conditions (Jiménez *et al.*, 2012c), in this case these not lead to a gel
486 formation. No significant differences were found among the Newtonian viscosity values
487 of the different formulations, despite the different total solid contents. In this sense, it is
488 remarkable that the composition of continuous phase is the same in all cases and the
489 volume concentration of the nanoliposomes is relatively low to affect notably the
490 sample viscosity.

491 The change from newtonian to shear thickening behaviour took place at a shear
492 rate ranging between 238-291 s⁻¹, regardless the type of sample. From these shear rate
493 values, the experimental data were fitted to the Ostwal-de-Waele model (power law).
494 The flow behaviour index (n) and the consistency index (k) of film forming dispersions
495 are shown in Table 3. No significant differences in n values, were found for the different
496 samples; these values being higher than 1, as corresponds to dilatant fluids and the
497 consistency index was also similar for all formulations.

498 In conclusion, small differences were found between the different film forming
499 dispersions concerning their rheological behaviour and only a decrease of their surface
500 tension was observed for those containing lipids due to the surfactant action of lecithin.

501

502 **3.3. Characterization of the films**

503 **3.3.1. Structural and mechanical properties**

504 Despite the small size of liposomes obtained in aqueous dispersion, when they are
505 incorporated into the film forming dispersions, the changes in the aqueous environment
506 and the establishment of interactions, mainly between surfactants and proteins
507 (Erickson, 1990), can promote significant changes in the structure of lipid particles. In
508 fact the mean size of particles increased when liposomes were incorporated in the film
509 forming dispersions and it could not be measured with the available equipment because
510 they were out the measure range.

511 A positive aspect of the essential oil incorporation as nanoliposomes was the
512 inhibition of the oil evaporation during the film drying step, which supposes a decrease
513 of the film thickness by the loss of solids, when a constant of solids per surface area was
514 poured in the plate to obtain de film. This has been previously observed in previous
515 works (Sánchez-González *et al.* 2010ab) and supposes the loss of potentially active
516 compounds of the film. Table 4 shows the values of the film's thickness, where the
517 increase of this parameter when nanoliposomes were incorporated can be observed, on
518 the contrary that occurs when free essential oil was incorporated in the film. This
519 increase confirms that, not only essential oil was not evaporated but also that the
520 arrangement of the polymer chains with lipids is more open probably due to a different
521 coupling of the components on the basis of the developed interactions.

522 Figure 2 shows the SEM micrographs of the cross section of control film and those
523 containing liposomes. Control film showed a quite homogeneous structure, but coarser
524 than that obtained by Jiménez *et al.* (2012c) for films with the same composition. In this
525 work, the authors prepared the film forming dispersions by applying a homogenization
526 step, using a rotor-stator equipment, at 95°C. The high temperature and the shear stress
527 promoted denaturation of the protein and the interaction between polymers, which
528 favours the formation of a more homogenous blend.

529 When control samples are compared with those containing lipids, a much coarser
530 structure is observed for the latter, which agrees with the increase of size of
531 nanoliposomes when incorporated to the film forming dispersions (data not showed)

532 and the possibly progress of this increase during the film drying step. During this step,
533 as the water of the system is being removed phase transitions occurs in the lipid
534 association structures which may promote the break of liposomes and the re-
535 restructuration of the molecule association, even giving rise to inverted structures
536 (Krog, 1990; Larsson, K., & Dejmek, 1990). In fact voids of different sizes can be
537 observed in the matrix, which can be associated to the presence of the lipid droplets
538 interrupting the matrix continuity in a size higher than nano-scale.

539 From the analysis of the stress-Hencky strain curves, elasticity modulus (EM),
540 tensile strength (TS) and elongation at break (E) were determined for each film sample.
541 According to McHugh & Krochta (1994), these parameters are very useful for
542 describing the mechanical properties of a film, and are closely related with its internal
543 structure. Table 4 shows the obtained values for each sample. Film without liposomes
544 presented the highest EM value, in comparison with nanoliposome containing films.
545 The addition of nanoliposomes introduces discontinuities in the matrix, as commented
546 on above, which affects significantly the mechanical resistance of films. The same
547 behaviour is observed for TS values. Considering the EM and TS values of control film
548 it is remarkable that there is a great difference between these values and those obtained
549 obtained by Jiménez *et al.* (2012c) using the same formulation starch-sodium caseinate,
550 but by applying a heat-homogenization step before the film casting. This could provoke
551 a reduction the mechanical resistance and extensibility of the obtained structure.

552 Among films containing nanoliposomes, for rapeseed liposomes, elastic modulus
553 significantly decreased when essential oil or limonene are present in the film which
554 could be due to a different release of this compounds in the matrix from liposomes.

555 As concerns extensibility of the films (E), these can be considered few extensible,
556 in comparison with other films in which starch were blended with other polymers (Phan
557 The, Debeaufort, Voilley & Luu, 2009; Jiménez *et al.*, 2012bc). This low extensibility
558 can be related with the kind of structure generated where the slippage of the chains
559 during the film stretching is more difficult. When heat-homogenization is was applied to
560 starch-sodium caseinate films with the same composition, extensibility is almost 2.5
561 times higher probably due to the heat induced unfolding of proteins and the more linear
562 entanglement of the chains in the matrix. In this work the heat-homogenization step was
563 not applied to avoid the rupture of nanoliposomes, thus losing the active compounds.

564

565 **3.3.2. Optical properties**

566 Spectral distribution curves of Ti parameters are plotted in Figure 3. In general,
567 high values of Ti are associated with greater film homogeneity, which gives rise to more
568 transparent films. On the contrary, lower values of Ti are related with a higher opacity
569 of the films. As observed in Figure 3, control film was the most transparent with high
570 values of Ti, in agreement with that reported in previous works for starch and sodium
571 caseinate (Fabra *et al.*, 2009; Jiménez *et al.*, 2012a). The addition of nanoliposomes
572 decreased the transparency of films regardless the type of lecithin and the antimicrobial
573 mainly at low wavelength. This fact is due, in part, to the natural brown colour of
574 lecithins. This produces the absorption of the blue and green light (low wavelength)
575 thus giving rise to a yellow-brown colour in the films. The presence of a dispersed
576 phase in the matrix also contributes to the decrease in the Ti values.

577 The colour of films as a consequence of nanoliposomes addition, is shown in Table
578 4, in terms of lightness (L^*), chroma (C_{ab}^*) and hue (h_{ab}^*) parameters, for each
579 formulation. L^* and C_{ab}^* values for control film varied significantly by the
580 incorporation of nanoliposomes. Incorporation of nanoliposomes provoked a decrease
581 the lightness and the hue and an increase of chroma, due to the colour of lecithins. The
582 film colour become more vivid a redder by the action of lecithin liposomes. To estimate
583 colour differences, ΔE were calculated between control film and the films containing
584 nanoliposomes. These values ranged between 25 and 29, thus indicating that there is a
585 relevant difference of colour between films. Nevertheless no notable differences were
586 found among in films containing nanoliposomes since there are no significant
587 differences in their colour parameters.

588

589 3.3.3. Fourier transform infrared spectroscopy

590 Figure 4A shows the FTIR spectra of the films without and with nanoliposomes
591 and Figure 4B the corresponding spectra of each one of film components, in order to
592 compare the main characteristics peaks of the different components and films. The
593 broad band located at 3300 cm^{-1} corresponds with vibration modes of OH-groups from
594 the absorbed water (García, Famá, Dufresne, Aranguren & Goyanes, 2009) and from the
595 polymers themselves (Bourtoom & Chinnan, 2008; Pereda, Amica, Rácz & Marcovich,
596 2011). The peaks located at 2854 and 2923 cm^{-1} are related with vibration of $-\text{CH}_2$ and
597 $-\text{CH}_3$ groups (axial carbon-hydrogen bond) (Zhang *et al.*, 2012). The band at 1690 - 1590
598 cm^{-1} corresponds to the amide I vibrations, which is common to proteins (Pereda,
599 Aranguren & Marcovich, 2008; Pereda *et al.*, 2011), as can be seen in Figure 4B for

600 sodium caseinate. Other main peak observed in Figure 4A, which has been associated
601 with C-O stretching vibrations (Zhang *et al.*, 2012), appeared at 1022 cm⁻¹.

602 FTIR spectra of the films were very similar, as correspond to their similar
603 composition. Nevertheless, some differences can be drawn. The main difference is the
604 higher intensity of the peak at 1022 cm⁻¹ in films containing nanoliposomes in
605 comparison with the control. As can be observed, in Figure 4B, lecithins presented a
606 broad band around this wavenumber, thus explaining the greater intensity observed in
607 Figure 4A for films containing nanoliposomes. The intensity of peaks at 2854 and 2923
608 cm⁻¹ also increased with nanoliposomes addition, in agreement with spectra observed in
609 Figure 4B for lecithins and antimicrobial compounds. For films with nanoliposomes,
610 Figure 4A also shows a little peak at 1746 cm⁻¹ which correspond to the C=O stretching
611 (Tantipolphan, Rades, McQuillan & Medlicott, 2007). This group is located between
612 hydrophobic tails and hydrophilic head group of the lecithin molecule. Nevertheless, no
613 displacement of peaks in the film spectra with respect to the characteristic wavelength
614 found for each isolated compound was observed, which indicates that no specific
615 interactions among components can be detected from FTIR spectra.

616

617 **3.3.4. Antimicrobial activity against *Listeria monocytogenes***

618 Figures 5A and 5B show the growth curves of *Listeria monocytogenes* on TSA
619 medium without film and on those coated with the different films. Bacteria population
620 increases from 3 to 8 logs CFU/cm² at the end of the storage period. The slightly greater
621 microbial growth in plates coated with the different films than in uncoated one can be
622 observed in Figures 5A and B. This indicates that they did not have antimicrobial
623 activity, as expected for starch-NaCas film (control), while contribute to the bacteria
624 nutrients as a consequence of its composition (protein and starch). The incorporation of
625 nanoliposomes did not improve the antimicrobial capacity of films, regardless the type
626 of lecithin and the potentially antimicrobial compound. Only orange oil-soy lecithin
627 nanoliposomes containing film seemed to present a little activity at the end of the
628 storage (day 7). In this case, some more days of analysis would be necessary to evaluate
629 if there is a significant antimicrobial activity. These results could be attributed to the
630 encapsulation of the active compounds in liposomes, which inhibit their release to the
631 plate surface and to a low antimicrobial activity of limonene and orange essential oil.
632 Similar results were reported by Imran (Imran, 2011) since he found that the release of
633 bioactive compounds entrapped onto nanoliposomes is a relatively long process.

634 Moreover this study revealed that nanoliposome composition is an important factor to
635 take into account to control the release of active compounds. In addition, Imran, Revol-
636 Junelles, René, Jamshidian, Akhtar, Arab-Tehrany, Jacquout & Desobry (2012)
637 observed that the highest antilisterial activity corresponded with films containing both
638 free and encapsulated antimicrobial compound. This result demonstrates that at initial
639 time it is necessary a little amount of free bioactive compound to avoid microbial
640 growth until it was released from the nanoliposomes. Concerning differences observed
641 between antilisterial activity of films with limonene and orange oil nanoliposomes,
642 previous studies reported also a greater effectiveness of the essential oils in terms of
643 antimicrobial activity than the mix of the major components or pure terpenes (Gill *et al.*
644 2002; Mourey & Canillac 2002). Minor components therefore play an important role,
645 and synergism phenomena occur.

646

647 **4. CONCLUSIONS**

648

649 The incorporation of potentially antimicrobial volatile compounds (orange
650 essential oil and limonene) to starch-sodium caseinate blend films was carried out in a
651 effective way to avoid the losses of volatile compounds during the film drying step.
652 Nanoliposomes of soy and rapeseed lecithins were obtained by sonication of their water
653 dispersions. Incorporation of the essential oil and limonene to the liposomes was also
654 effective by using the same method. The addition of lipids in the polymeric matrix
655 supposed a decrease of the mechanical resistance and extensibility of the films. The
656 natural colour of lecithin conferred a loss of lightness, a chroma gain and a redder hue
657 to the films, which were also less transparent than the control one, regardless the
658 lecithin and volatile lipid considered. The possible antimicrobial activity of the films
659 containing orange essential oil or limonene was not observed, which could be due to
660 their low antilisterial activity or to the inhibition effect of the encapsulation which
661 difficult their release from the matrix.

662

663

664 **REFERENCES**

- 665 - Ackman, R.G. (1998). Remarks on official methods employing boron trifluoride in the
666 preparation of methyl esters of the fatty acids of fish oils. *Journal of the American Oil*
667 *Chemists's Society*, 75, 541-545.
- 668 - Arab Tehrany, E., Kahn, C.J.F., Baravian, C., Maherani, B., Belhaj, N., Wang, X., &
669 Linder (2012). Elaboration and characterization of nanoliposome made of soy; rapeseed
670 and salmon lecithins: Application to cell culture. *Colloids and Surfaces B:*
671 *Biointerfaces*, 95 (15), 75-81.
- 672 - ASTM (2001) Standard test method for tensile properties of thin plastic sheeting.
673 Standard D882. *Annual Book of American Standard Testing Methods*; American Society
674 for Testing and Materials: Philadelphia, PA; pp 162-170.
- 675 - Averous, L., Moro, L., Dole, P., & Fringant. (2000). Properties of thermoplastic
676 blends:starch-polycaprolactone. *Polymer*, 41(11), 4157-4167.
- 677 - Bakkali, F., Averbeck, S., Averbeck, D., & Idaomar, I. (2008). Biological effects of
678 essential oils: A review. *Food and Chemical Toxicology*, 46, 446-475.
- 679 - Bourtoom, T., & Chinnan, M.S. (2008). Preparation and properties of rice starch-
680 chitosan blend biodegradable film. *LWT-Food Science and Technology*, 41 (9), 1633-
681 1641.
- 682 - Bravin, B., Peressini, D., & Sensidoni, A. (2004). Influence of emulsifier type and
683 content on functional properties of polysaccharide lipid-based edible films. *Journal of*
684 *Agricultural and Food Chemistry*, 52 (21), 6448-6455.
- 685 - Chansiri, G., Lyons, R.T., Patel, M.V., & Hem, S.L. (1999). Effect of surface charge
686 on the stability of oil/water emulsions during steam sterilization. *Journal of*
687 *Pharmaceutical Sciences*, 88 (4), 454-458.
- 688 - Chick, J., & Ustunol, Z. (1998). Mechanical and barrier properties of lactic acid and
689 rennet precipitated casein-based edible films. *Journal of Food Science*, 63 (6), 1024-
690 1027.
- 691 - Christianson, D. D., & Bagley, E. B. (1983). Apparent viscosity of dispersions of
692 swollen cornstarch granules. *Cereal Chemistry*, 60 (2), 116-121.
- 693 - Clément, L., Hurel, C., & Marmier, N. (2013). Toxicity of TiO₂ nanoparticles to
694 cladocerans, algae, rotifers and plants – Effects of size and crystalline structure.
695 *Chemosphere*, 90 (3), 1083-1090.

- 696 - Edris, A.E., & Farrag, E.S. (2003). Antifungal activity of peppermint and sweet basil
697 essential oils and their major aroma constituents on some plant pathogenic fungi from
698 the vapor phase. *Food/Nahrung*, 47 (2), 117-121.
- 699 - Erickson, E. (1990). *Lipid-protein interactions*. In Larson, K., & Friberg, S. E. (Eds.),
700 Food emulsions. New York/Basel: Marcel Dekker, Inc.
- 701 - Fabra, M.J., Jiménez, A., Atarés, L., Talens, P., & Chiralt, A. (2009). Effect of fatty
702 acids and beeswax addition on properties of sodium caseinate dispersions and films.
703 *Biomacromolecules*, 10 (6), 1500-1507.
- 704 - Famá, L., Goyanes, S., & Gerschenson, L. (2007). Influence of storage time at room
705 temperature on the physicochemical properties of cassava starch films. *Carbohydrate*
706 *Polymers*, 70 (3), 265-273.
- 707 - Fang, J., & Fowler, P. (2003). The use of starch and its derivatives as biopolymer
708 sources of packaging materials. *Food, Agriculture & Environment*, 1(3-4), 82-84.
- 709 - Fernández, L., Díaz de Apodaca, E., Cebrián, M., Villarán, M.C., & Maté, J.I. (2006).
710 Effect of the unsaturation degree and concentration of fatty acids on the properties of
711 WPI-based edible films. *European Food Research and Technology*, 224 (4), 415-420.
- 712 - Fisher, K., & Phillips, C.A. (2006). The effect of lemon, orange and bergamot
713 essential oils and their components on the survival of *Campylobacter jejuni*,
714 *Escherichia coli* O157, *Listeria monocytogenes*, *Bacillus cereus* and *Staphylococcus*
715 *aureus* in vitro and in food systems. *Journal of Applied Microbiology*, 101 (6), 1232-
716 1240.
- 717 - Gallucci, M.N., Oliva, M., Casero, C., Dambolena, J., Luna, A., Zygadlo, J., & Demo,
718 M. (2009). Antimicrobial combined action of terpenes against the food-borne
719 microorganisms *Escherichia coli*, *Staphylococcus aureus* and *Bacillus cereus*. *Flavour*
720 *and Fragrance Journal*, 24 (6), 348-354.
- 721 - García, N.L., Famá, L., Dufresne, A., Aranguren, M., & Goyanes, S. (2009). A
722 comparison between the physico-chemical properties of tuber and cereal starches. *Food*
723 *Research International*, 42 (8), 976-982.
- 724 - Gill, A.O., Delaquis, P., Russo, P., & Holley, R.A. (2002). Evaluation of antilisterial
725 action of cilantro oil on vacuum packed ham. *International Journal of Food*
726 *Microbiology*, 73 (1), 83-92.

- 727 - Han, J.H. (2002). Protein-based edible films and coatings carrying antimicrobial
728 agents. In Gennadios, A. (Ed.), *Protein-based films and coatings* (pp. 485-500). Boca
729 Raton: CRC Press.
- 730 - Hsiao, I.L., & Huang, Y.J. (2011). Effects of various physicochemical characteristics
731 on the toxicities of ZnO and TiO₂ nanoparticles toward human lung epithelial cells.
732 *Science of the Total Environment*, 409 (7), 1219-1228.
- 733 - Hutchings, J.B. (1999). *Food and Colour Appearance*, Second Edition. Gaithersburg,
734 Maryland: Chapman and Hall Food Science Book, Aspen Publication.
- 735 - Imran, M. (2011). Active packaging containing nano-vectorized antimicrobial
736 peptides. PhD Thesis. Institute National Polytechnique de Lorraine (Université de
737 Lorraine).
- 738 - Imran, M., Revol-Junelles, A.M., René, N., Jamshidian, M., Akhtar, M.J., Arab-
739 Tehrani, E., Jacquot, M., & Desobry, S. (2012). Microstructure and physico-chemical
740 evaluation of nano-emulsion-based antimicrobial peptides embedded in bioactive
741 packaging films. *Food Hydrocolloids*, 29 (2), 407-419.
- 742 - Iturriaga, L., Olabarrieta, I., & Martínez de Marañón, I. (2012). Antimicrobial assays
743 of natural extracts and their inhibitory effect against *Listeria innocua* and fish spoilage
744 bacteria, after incorporation into biopolymer edible films. *International Journal of Food*
745 *Microbiology*, 158 (1), 58-64.
- 746 - Jiménez, A., Fabra, M.J., Talens, P., & Chiralt, A. (2012a). Effect of re-crystallization
747 on tensile, optical and water vapour barrier properties of corn starch films containing
748 fatty acids. *Food Hydrocolloids*, 26 (1), 302-310.
- 749 - Jiménez, A., Fabra, M.J., Talens, P., & Chiralt, A. (2012b). Influence of
750 hydroxypropylmethylcellulose addition and homogenization conditions on properties
751 and ageing of corn starch based films. *Carbohydrate Polymers*, 89 (2), 676-686.
- 752 - Jiménez, A., Fabra, M.J., Talens, P., & Chiralt, A. (2012c). Effect of sodium caseinate
753 on properties and ageing behaviour of corn starch based films. *Food Hydrocolloids*, 29
754 (2), 265-271.
- 755 - Kristo, E., Koutsoumanis, K.P., & Biliaderis, C.G. (2008). Thermal, mechanical and
756 water vapor barrier properties of sodium caseinate films containing antimicrobials and
757 their inhibitory action on *Listeria monocytogenes*. *Food Hydrocolloids*, 22 (3), 373-386.

- 758 - Krog, N. J. (1990). *Food emulsifiers and their chemical and physical properties*. In
759 Larson, K., & Friberg, S. E. (Eds.), *Food emulsions*. New York/Basel: Maecer Dekker,
760 Inc.
- 761 - Lankveld, D.P.K., Oomen, A.G., Krystek, P., Neigh, A., Troost-de Jong, A.,
762 Noorlander, C.W., Van Eijkeren, J.C.H., Geertsma, R.E., & De Jong, W.H. (2010). The
763 kinetics of the tissue distribution of silver nanoparticles of different sizes. *Biomaterials*,
764 31 (32), 8350-8361.
- 765 - Larsson, K., & Dejmeek, P. (1990). *Crystal and liquid crystal structures of lipids*. In
766 Larson, K., & Friberg, S. E. (Eds.), *Food emulsions*. New York/Basel: Maecer Dekker,
767 Inc.
- 768 - Leshem, Y., Landau, E., & Deutsch, M. (1988). A monolayer model study of surface
769 tension-associated parameters of membrane phospholipids: Effect of unsaturation of
770 fatty acyl tails. *Journal of Experimental Botany*, 39 (2), 1679–1687.
- 771 - López, O. V., García, M. A., & Zaritzky, N. E. (2008). Film forming capacity of
772 chemically modified corn starches. *Carbohydrate Polymers*, 73(4), 573–581.
- 773 - López, O., & García, M.A. (2012). Starch films from a novel (*Pachyrhizus ahipa*) and
774 conventional sources: Development and characterization. *Materials Science and*
775 *Engineering*, 32 (7), 1931-1940.
- 776 - Lourdin, D., Della Valle, G., & Colonna, P. (1995). Influence of amylose content on
777 starch films and foams. *Carbohydrate Polymers*, 27 (4), 261-270.
- 778 - Maran, J.P., Sivakumar, V., Sridhar, R., & Immanuel, V.P. (2013). Development of
779 model for mechanical properties of tapioca starch based edible films. *Industrial Crops*
780 *and Products*, 42, 159-168.
- 781 - McHugh, T. H., & Krochta, J. M. (1994). Water vapour permeability properties of
782 edible whey protein–lipid emulsion films. *Journal of the American Oil Chemists*
783 *Society*, 71 (3), 307–312.
- 784 - McSweeney, S.L., Healy, R., & Mulvihill, D.M. (2008). Effect of lecithin and
785 monoglycerides on the heat stability of a model infant formula emulsion. *Food*
786 *Hydrocolloids*, 22 (5), 888-898.

- 787 - Mourey, A., & Canillac, N. (2002). Anti-*Listeria monocytogenes* activity of essential
788 oils components of conifers. *Food Control*, 13 (4-5), 289-292.
- 789 - Paes, S. S., Yakimets, I., & Mitchell, J. R. (2008). Influence of gelatinization process
790 on functional properties of cassava starch films. *Food Hydrocolloids*, 22, 788–797.
- 791 - Pagella, C., Spigno, G., & De Faveri, D. M. (2002). Characterization of starch based
792 edible coatings. *Food and Bioproducts Processing*, 80(3), 193–198.
- 793 - Peker, S.M., & Helvacı, Ş.Ş. (2007). Concentrated suspensions. In Peker, S.M.,
794 Helvacı, Ş.Ş., Yener, H.B., İkizler, B., & Alparsian, A. (Eds.), *Solid-liquid two phase*
795 *flow* (pp. 167-243). Amsterdam: Elsevier.
- 796 - Pereda, M., Aranguren, M.I., & Marcovich, N.E. (2008). Characterization of
797 chitosan/caseinate films. *Journal of Applied Polymer Science*, 107 (2), 1080–1090.
- 798 - Pereda, M., Amica, G., Rácz, I., & Marcovich, N.E. (2011). Structure and properties
799 of nanocomposite films based on sodium caseinate and nanocellulose fibers. *Journal of*
800 *Food Engineering*, 103 (1), 76-83.
- 801 - Pérez-Gago, M.B., & Krochta, J.M. (2001). Lipid particle size effect on water vapor
802 permeability and mechanical properties of whey protein/beeswax emulsion films.
803 *Journal of Agricultural and Food Chemistry*, 49 (2), 996-1002.
- 804 - Phan The, D., Debeaufort, F., Voilley, A., & Luu, D. (2009). Biopolymer interactions
805 affect the functional properties of edible films based on agar, cassava starch and
806 arabinoxylan blends. *Journal of Food Engineering*, 90 (4), 548-558.
- 807 - Piccirillo, C., Demiray, S., Silva Ferreira, A.C., Pintado, M.E., & Castro, P.M.L.
808 (2013). Chemical composition and antibacterial properties of stem and leaf extracts
809 from Ginja cherry plant. *Industrial Crops and Products*, 43, 562-569.
- 810 - Ruiz-Navajas, Y., Viuda-Martos, M., Sendra, E., Perez-Alvarez, J.A., & Fernández-
811 López, J. (2013). In Vitro antibacterial and antioxidant properties of chitosan edible
812 films incorporated with *Thymus moroderi* or *Thymus piperella* essential oils. *Food*
813 *Control*, 30 (2), 386-392.
- 814 - Sánchez-González, L., Cháfer, M., Chiralt, A., & González-Martínez, C. (2010a).
815 Physical properties of chitosan films containing bergamot essential oil and their
816 inhibitory action on *Penicillium italicum*. *Carbohydrate Polymers*, 82 (2), 277-283.

- 817 - Sánchez-González, L., González-Martínez, C., Chiralt, A., & Cháfer, M. (2010^b).
818 Physical and antimicrobial properties of chitosan-tea tree essential oil composite films.
819 *Journal of Food Engineering*, 98(4), 443-452.
- 820 - Sánchez-González, L., Vargas, M., González-Martínez, C., Cháfer, M., & Chiralt, A.
821 (2011a). Use of essential oils in bioactive edible coatings: A review. *Food Engineering*
822 *Reviews*, 3 (1), 1-16.
- 823 - Sánchez-González, L., Cháfer, M., Hernández, M., Chiralt, A., & González-Martínez,
824 C. (2011b). Antimicrobial activity of polysaccharide films containing essential oils.
825 *Food Control*, 22 (8), 1302-1310.
- 826 - Sandasi, M., Leonard, C.M., & Viljoen, A.M. (2008). The effect of five common
827 essential oil components on *Listeria monocytogenes* biofilms. *Food Control*, 19 (11),
828 1070-1075.
- 829 - Smith-Palmer, A., Stewart, J., & Fyfe, L. (2001). The potential application of plant
830 essential oils as natural food preservatives in soft cheese. *Food Microbiology*, 18 (4),
831 463-470.
- 832 - Soliva-Fortuny, R., Rojas-Graü, M.A., & Martín-Belloso, O. (2012). Polysaccharide
833 coatings. In Baldwin, E.A., Hagenmaier, R., & Bai, J. (Eds.), *Edible coatings and films*
834 *to improve food quality* (pp. 103-136). Boca Raton: CRC Press.
- 835 - Tantipolphan, R., Rades, T., McQuillan, A.J., & Medlicott, N.J. (2007). Adsorption of
836 bovine serum albumin (BSA) onto lecithin studied by attenuated total reflectance
837 Fourier transform infrared (ATR-FTIR) spectroscopy. *International Journal of*
838 *Pharmaceutics*, 337 (1-2), 40-47.
- 839 - Walstra, P. (2003). *Physical Chemistry of Foods*. Marcel Dekker, Inc., New York.
- 840 - Ye, C.L., Dai, D.H., & Hu, W.L. (2013). Antimicrobial and antioxidant activities of
841 the essential oil from onion (*Allium cepa* L.). *Food Control*, 30 (1), 48-53.
- 842 - Zhang, H.Y., Arab Tehrani, E., Kahn, C.J.F., Ponçot, M., Linder, M., & Cleymand, F.
843 (2012). Effects of nanoliposomes based on soy, rapeseed and fish lecithins on chitosan
844 thin films designed for tissue engineering. *Carbohydrate Polymers*, 88 (2), 618-627.
- 845 - Zhou, J., Ren, L., Tong, J., Xie, L., & Liu, Z. (2009). Surface esterification of corn
846 starch films: reaction with dodecyl succinic anhydride. *Carbohydrate Polymers*,
847 78(4), 888-893.

848 - Zhou, J., Zhang, J., Ma, Y., & Tong, J. (2008). Surface photo-crosslinking of corn
849 starch sheets. *Carbohydrate Polymers*, 74(3), 405-410.

850

851

852

853

854

855

856

857

858

859

860

861

862

863

864

865

866

867

868

869

870

871

872

873

874

875

876

877

878

879

880

881

882 **Table 1. Main fatty acids composition of rapeseed and soy lecithins.**

Fatty acids	Rapeseed lecithin		Soy lecithin	
	%	SD	%	SD
C14	-	-	-	-
C15	-	-	-	-
C16	7.41	0.01	17.07	0.48
C17	-	-	-	-
C18	1.31	0.00	3.32	0.16
C20	0.36	0.01	-	-
C21	-	-	-	-
C22	0.21	0.02	0.43	0.04
C23	-	-	-	-
SFA	9.29		20.82	
C15:1	-	-	-	-
C16:1	0.33	0.01	-	-
C17:1	-	-	-	-
C18:1n9	56.51	0.04	21.49	0.47
C20:1n11	0.72	0.04	-	-
C22:1n9	0.25	0.03	-	-
MUFA	57.81		21.49	
C18:2n6	26.32	0.04	52.27	0.36
C18:2n3	6.60	0.01	5.41	0.04
C20:2n6	-	-	-	-
C20:3n6	-	-	-	-
C20:3n3	-	-	-	-
C20:4n6	-	-	-	-
C20:5n3 (EPA)	-	-	-	-
C22:4n6	-	-	-	-
C22:5n3	-	-	-	-
C22:6n3 (DHA)	-	-	-	-
PUFA	32.92		57.68	

883

884

885

886

887

888

889

890

891

892

893

894

895 **Table 2. Particle size, electrophoretic mobility and surface tension of aqueous**
 896 **nanoliposomes solutions.**

	Particle size (nm)	μE ($\mu\text{m}\cdot\text{cm}/\text{V}\cdot\text{s}$)	ST ($\text{mN}\cdot\text{m}^{-1}$)
Rap	146 (1) ^a	-3.21 (0.01) ^a	26.8 (0.5) ^a
Rap-lim	150 (3) ^a	-3.36 (0.03) ^b	27.7 (0.2) ^{ab}
Rap-oil	148 (2) ^a	-3.31 (0.02) ^b	27.9 (0.4) ^b
Soy	188 (5) ¹	-3.89 (0.07) ¹	31.6 (0.6) ¹
Soy-lim	175 (5) ²	-3.98 (0.03) ¹²	28.6 (0.7) ²
Soy-oil	159 (5) ³	-3.99 (0.02) ²	28.0 (1.0) ²

897 a-c: Different superscripts within the same column indicate significant differences among formulations
 898 containing rapeseed nanoliposomes ($p < 0.05$).

899 1-3: Different superscripts within the same column indicate significant differences among formulations
 900 containing soy nanoliposomes ($p < 0.05$).

901

902

903

904

905

906

907

908

909

910

911

912

913

914

915

916

917

918

919

920

921

922

923

924

925

Table 3. Surface tension and rheological properties of film forming dispersions.

	Newtonian viscosity ($\cdot 10^3$, Pa·s)	n	K ($\cdot 10^3$, Pa·sⁿ)	ST (mN·m⁻¹)
Control	5.7 (0.1) ^{ab1}	1.27 (0.01) ^{a1}	1.47 (0.07) ^{a1}	51.1 (0.1) ^{a1}
Rap	5.8 (0.2) ^a	1.24 (0.01) ^b	1.75 (0.14) ^b	44.9 (0.7) ^b
Rap-lim	5.4 (0.2) ^b	1.25 (0.01) ^{ab}	1.5 (0.1) ^a	43.8 (1.7) ^b
Rap-oil	5.7 (0.1) ^{ab}	1.24 (0.01) ^b	1.75 (0.06) ^b	43.6 (1.4) ^b
Soy	5.62 (0.04) ¹²	1.26 (0.01) ¹	1.52 (0.07) ¹	44.6 (1.2) ²
Soy-lim	5.5 (0.1) ¹²	1.25 (0.01) ¹	1.5 (0.1) ¹	46 (1) ²
Soy-oil	5.4 (0.2) ²	1.25 (0.01) ¹	1.6 (0.2) ¹	42.0 (0.3) ³

927

a-b: Different superscripts within the same column indicate significant differences among formulations containing rapeseed nanoliposomes ($p < 0.05$).

928

929

1-3: Different superscripts within the same column indicate significant differences among formulations containing soy nanoliposomes ($p < 0.05$).

930

931

932

933

934

935

936

937

938

939

940

941

942

943

944

945

946

947

948

949

950

951

952

953

954

955 **Table 4. Mechanical properties and colour of the obtained films.**

	EM (MPa)	TS (MPa)	E (%)	Thickness (µm)
Control	1900 (200) ^{a1}	27.6 (1.5) ^{a1}	2.9 (0.5) ^{a1}	55 (8) ^{a1}
Rap	1300 (200) ^b	8.0 (0.7) ^b	0.8 (0.2) ^b	63 (8) ^a
Rap-lim	700 (100) ^c	7.8 (0.4) ^b	2.0 (0.2) ^c	76 (11) ^b
Rap-oil	900 (200) ^c	7.1 (1.8) ^b	1.0 (0.3) ^b	89 (12) ^c
Soy	900 (100) ²	9.6 (1.9) ²	1.7 (0.6) ²	66 (7) ²
Soy-lim	1000 (100) ²	11 (2) ²	1.8 (0.6) ²	71 (11) ²
Soy-oil	860 (70) ²	9.6 (0.3) ²	1.7 (0.1) ²	81 (9) ³

	L*	C_{ab}*	h_{ab}*	ΔE
Control	88 (2) ^{a1}	8.8 (1.3) ^{a1}	95.4 (1.2) ^{a1}	--
Rap	74.5 (1.0) ^b	32.5 (0.6) ^b	82.6 (0.2) ^b	27.4
Rap-lim	74.6 (1.1) ^b	32 (1) ^b	83 (1) ^b	26.9
Rap-oil	74 (2) ^b	33 (1) ^b	82.7 (1.3) ^b	28.9
Soy	75 (1) ²	33.0 (0.5) ²	79.4 (0.2) ²	27.8
Soy-lim	77.8 (0.5) ²	30.8 (0.8) ³	81 (1) ²³	24.5
Soy-oil	75.9 (0.8) ²	31 (1) ²³	82 (1) ³	25.6

956 EM: Elastic modulus; TS: Tensile strength; E: Elongation at break. L*: Lightness, Cab*: Chroma; hab*:
 957 Hue; ΔE: Colour difference in comparison with control film.

958 a-c: Different superscripts within the same column indicate significant differences among formulations
 959 containing rapeseed nanoliposomes ($p < 0.05$).

960 1-3: Different superscripts within the same column indicate significant differences among formulations
 961 containing soy nanoliposomes ($p < 0.05$).

962

963

964

965

966

967

968

969

970

971

972

973

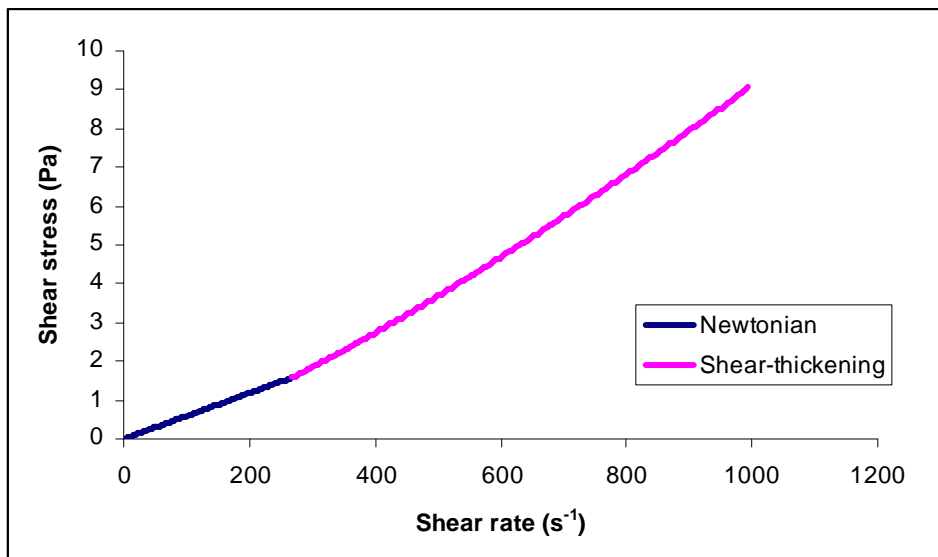
974

975

976

977

978

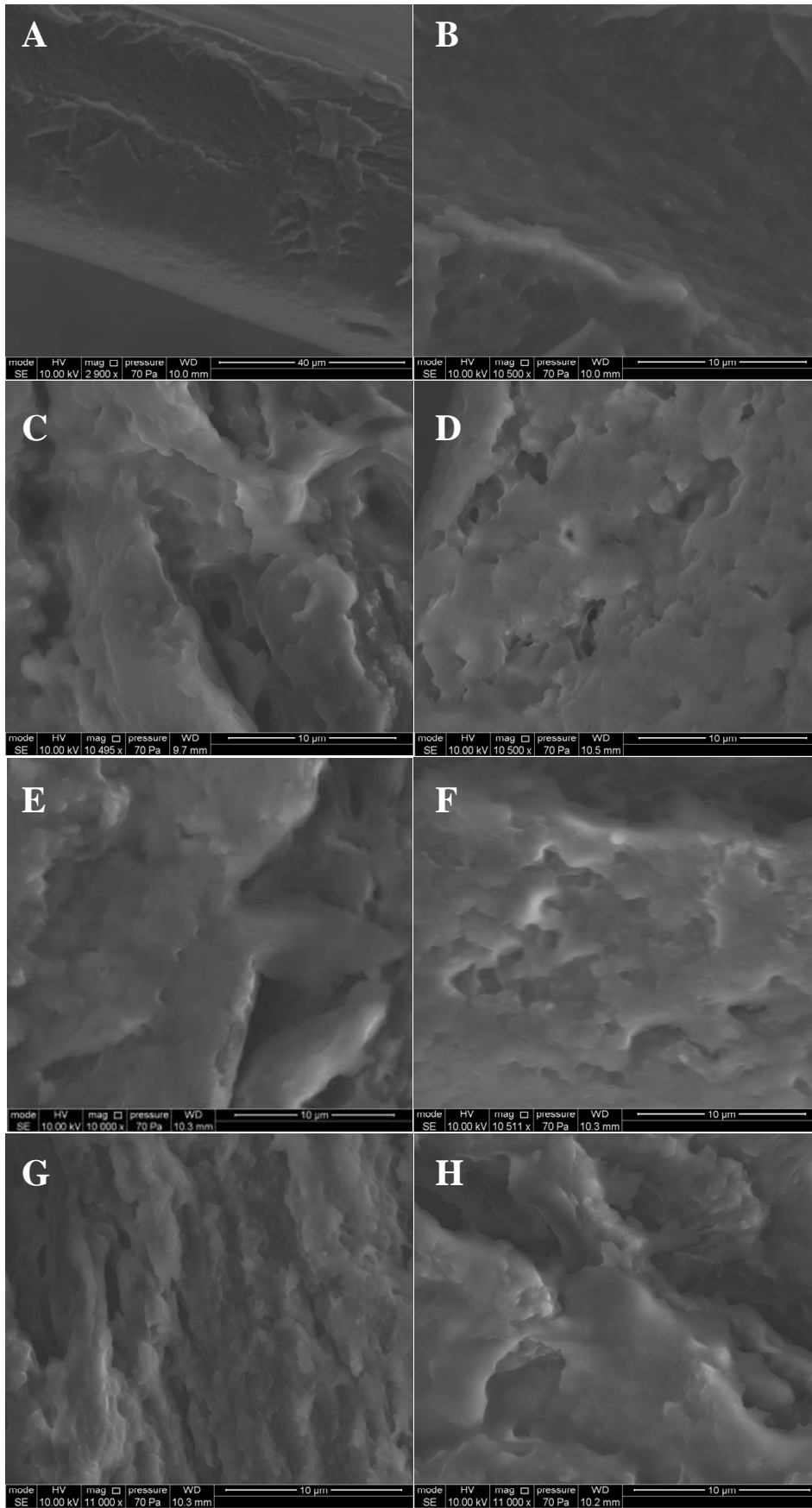


979

980 **Figure 1. Flow curve of control formulation (without nanoliposomes) showing the**

981 **change between newtonian and shear-thickening behaviour.**

982

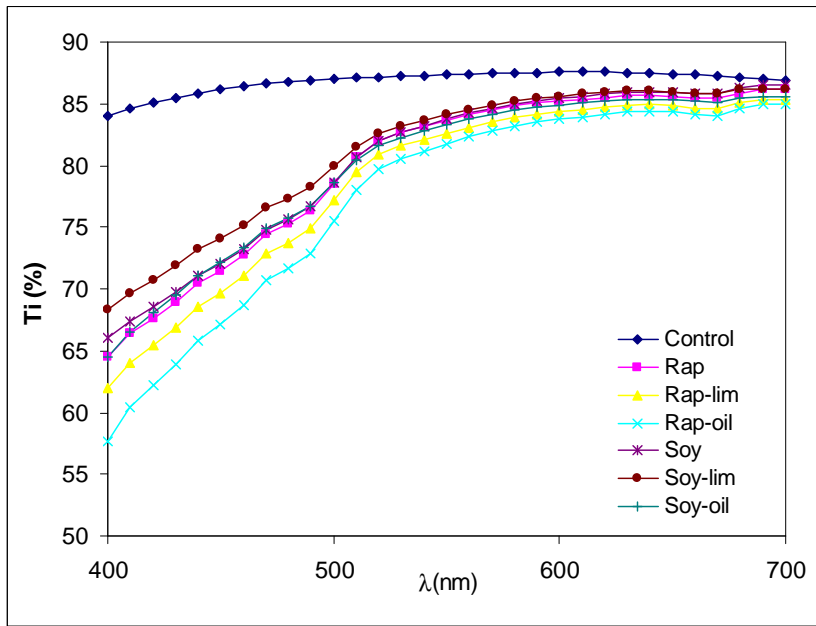


983

984

985

Figure 2. SEM micrographs of the cross-sections of the films. (A-B: Control, C:Rap, D: Rap-lim, E: Rap-oil, F: Soy, G: Soy-lim, H: Soy-oil).



986

987 **Figure 3.** Spectra of internal transmittance (Ti) of obtained films.

988

989

990

991

992

993

994

995

996

997

998

999

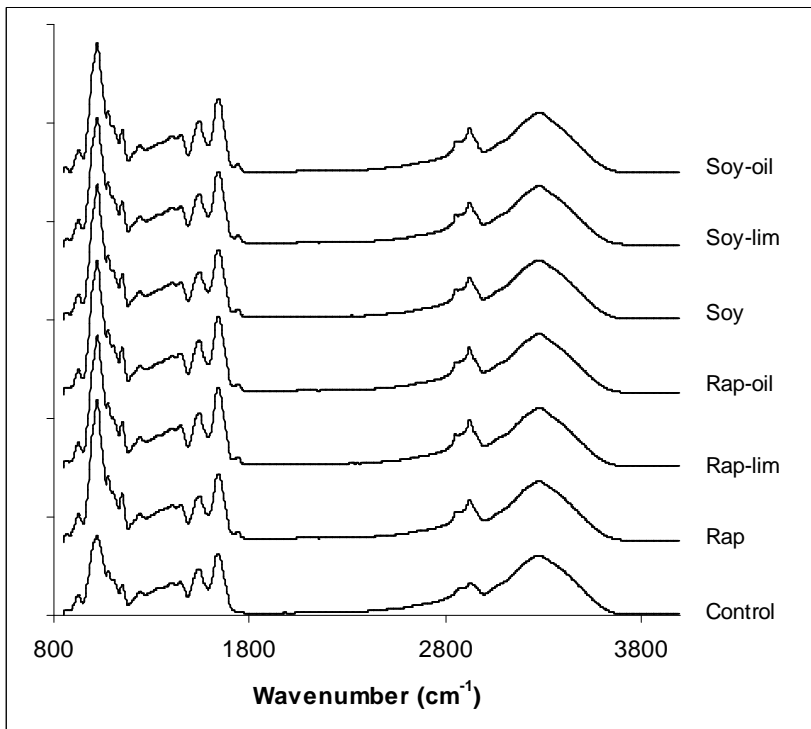
1000

1001

1002

1003

1004



1005

1006 **Figure 4A. FTIR spectra of the studied films.**

1007

1008

1009

1010

1011

1012

1013

1014

1015

1016

1017

1018

1019

1020

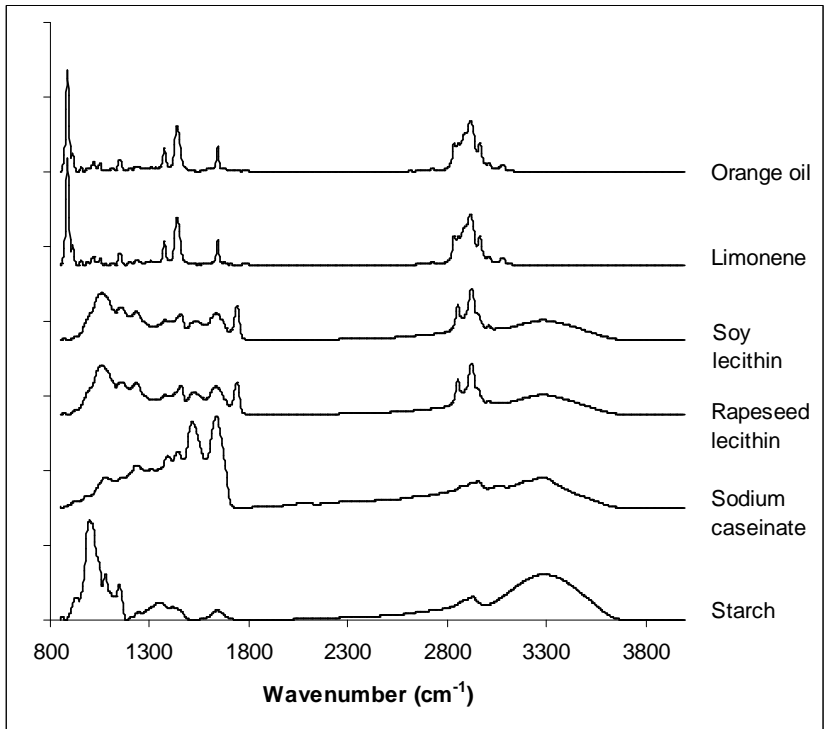
1021

1022

1023

1024

1025



1026

1027 **Figure 4B. FTIR spectra of isolated components of the films.**

1028

1029

1030

1031

1032

1033

1034

1035

1036

1037

1038

1039

1040

1041

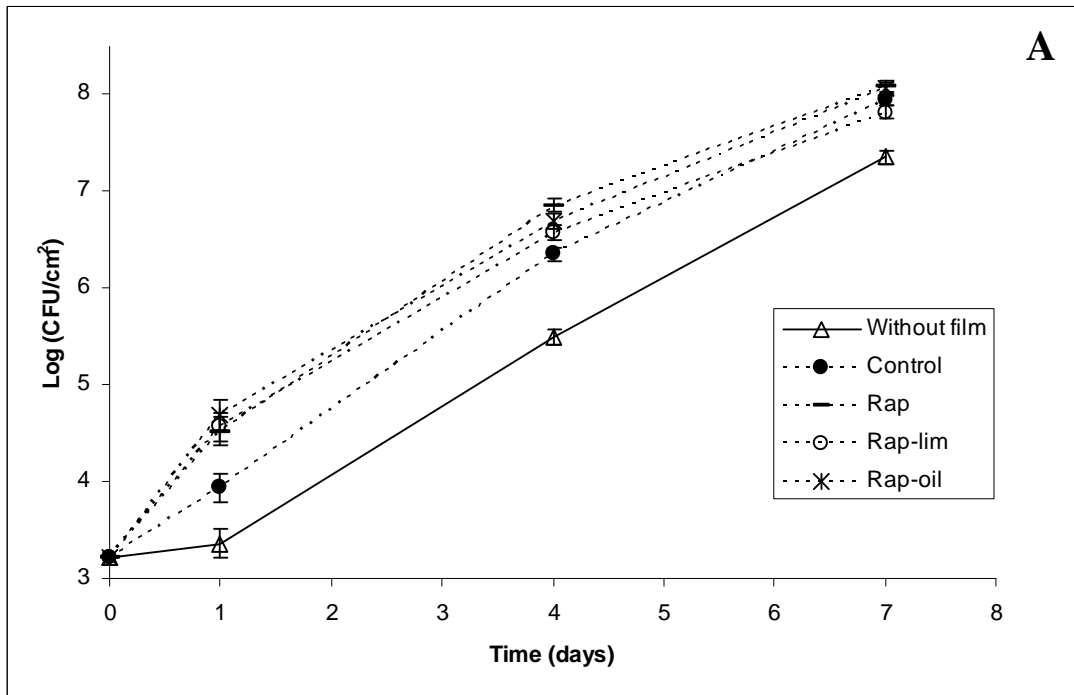
1042

1043

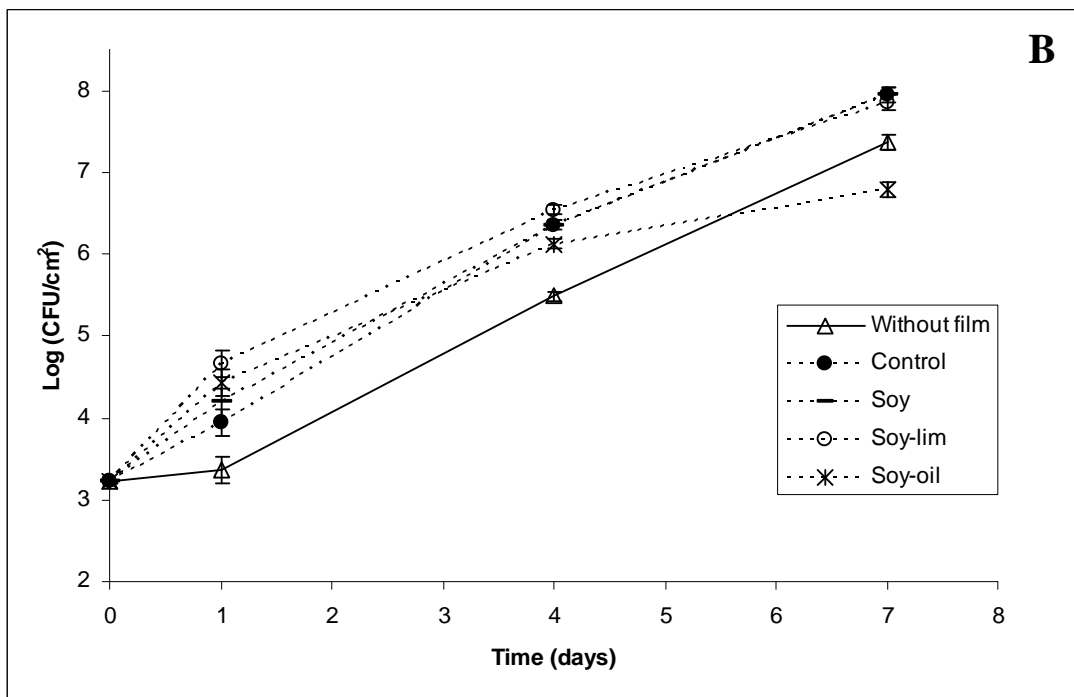
1044

1045

1046



1047



1048

1049 **Figure 5.** Microbial counts as a function of time for samples without films and
 1050 coated with the different films containing rapeseed liposomes (A) and soy
 1051 liposomes (B). Mean values and LSD intervals.

1052